

## Potential functionals versus density functionals

Attila Cangi,<sup>1</sup> E. K. U. Gross,<sup>1</sup> and Kieron Burke<sup>2</sup>

<sup>1</sup>Max Planck Institute of Microstructure Physics, Weinberg 2, 06120 Halle (Saale), Germany

<sup>2</sup>Department of Chemistry, University of California, Irvine, 1102 Natural Sciences 2, Irvine, California 92697-2025, USA

(Received 15 July 2013; published 4 December 2013)

Potential functional approximations are an intriguing alternative to density functional approximations. The potential functional that is dual to the Lieb density functional is defined and its properties are reported. The relationship between the Thomas-Fermi theory as a density functional and the theory as a potential functional is derived. The properties of several recent semiclassical potential functionals are explored, especially regarding their approach to the large particle number and classical continuum limits. The lack of ambiguity in the energy density of potential functional approximations is demonstrated. The density-density response function of the semiclassical approximation is calculated and shown to violate a key symmetry condition.

DOI: [10.1103/PhysRevA.88.062505](https://doi.org/10.1103/PhysRevA.88.062505)

PACS number(s): 31.15.E-, 71.15.Mb

### I. INTRODUCTION AND SUMMARY OF RESULTS

Kohn-Sham (KS) density functional theory (DFT) [1] has been a useful approach to dealing with electronic structure problems, with more than 10 000 papers per year currently published. The only approximation needed (in the nonrelativistic Born-Oppenheimer limit) is to the elusive exchange-correlation (XC) energy as a functional of the (spin) densities. While tremendous progress has been made in constructing clever approximations [2–5] over the last half-century, such approximations are generally unreliable and unsystematic and do not produce error estimates [6].

An alternative approach, and one that fits far better with traditional approaches to quantum mechanics, is to consider the electronic-structure problem as a functional of the one-body potential [7] rather than of the one-body density. However, useful approximations beyond the local approximation [1,8,9] are far more subtle and complex to construct, so almost no research has been done in this area, at either the formal or the practical level. Notable exceptions are the density-potential functional formulation of Englert [10] and the pioneering work by Yang, Ayers, and Wu [11], which pointed out the duality of density and potential functionals and thus produced a deeper understanding of the optimized effective potential method. More recently, Gross and Proetto [12] emphasized the relevance of the variational principle to potential functional theory (PFT). Our own recent work [13] is focused on the fundamentals of approximate PFT and was motivated by recent semiclassical potential functional approximations (PFAs) for simple model systems [14,15].

In the present work, we explain in detail the differences between potential and density functionals, show that certain well-known difficulties of DFT are avoided, and demonstrate the accuracy achievable in PFT calculations (but only for a model system, for which accurate PFAs have been derived [14,15]). First, we give a detailed account of the exact theory and compare it with DFT. In PFT, just as in quantum mechanics, we work within a Hilbert space with a well-defined ground-state wave function and energy *a priori* and therefore avoid the notoriously subtle issue of density-potential mapping that is required in DFT. Another difference from DFT is that, in PFT, there are two distinct ways of obtaining the total energy of an interacting system: via a direct evaluation

of the functional approximations or variationally through a minimization over trial potentials. We present a previously derived [13] expression for the universal potential functional that yields the total energy at the variational minimum (without having to do an actual minimization), if a key symmetry condition on the density-density response function is fulfilled.

Levy [16] and Lieb [17] extended the domain of the universal functional given in the original work of Hohenberg and Kohn (HK) [18]. The construction of the Lieb density functional involves a bifunctional of the density and potential. What is the analog in PFT? In Sec. II, we repeat this exercise in PFT to explicitly show that the naive expression for the universal potential functional suffices.

In practice, our results for the interacting case are not yet useful for an actual numerical calculation, because they require knowledge of the interacting density as a functional of the external one-body potential [12]. But all our results apply to a noninteracting system in some external one-body potential. As a result, we obtain an explicit expression for the noninteracting kinetic energy as a functional of the potential. This expression has the powerful feature that only the noninteracting density needs to be known as a functional of the external one-body potential to fully determine the noninteracting kinetic energy.

Conflating the results for the noninteracting case with the KS scheme for exchange and correlation allows us to solve the interacting many-body problem in a much more efficient way than in KS-DFT, because there is no need to resort to the KS orbitals. In fact, the KS potential becomes a functional of the external one-body potential and is determined via an alternative self-consistent cycle depicted in Sec. III. In principle, all this is exact; a practical realization requires nothing but a sufficiently accurate approximation to the noninteracting density as a functional of the external one-body potential.

To illustrate how all this works and contrast it with DFT, in Sec. IV, we reconstruct the simplest approximation, Thomas-Fermi (TF) theory. We show how it can be constructed in either the potential functional or the density functional formalism. The logic and derivations are completely different, but the final equations are the same. Thus TF theory can be seen as the forerunner of exact PFT just as easily as the forerunner of exact DFT.

The early attempts at density functional construction for the kinetic [19] and the exchange [20] energy begin with the local approximation and improve on it via a gradient expansion [1,18]. However, these approximations fail for localized systems, such as atoms, molecules, or even some bulk solids. This is due to the presence of evanescent regions that are separated by turning point surfaces, i.e., where the Fermi energy cuts the potential energy surface. In an earlier account [14] we explain how this failure can be understood by considering the expansion of the total energy in the large- $N$  limit, where  $N$  denotes the number of particles. This analysis also explains why generalized gradient approximations were eventually introduced. Furthermore, our analysis suggests that PFAs provide a systematic approach to functional construction. The expansion of the total energy of neutral atoms with respect to the atomic number [21,22] is probably the most prominent example of such expansions. Considering how accurately the coefficients of such expansions are reproduced by an approximation also gives a measure of the accuracy of a given approximation: we call an approximation asymptotically exact to the  $p$ th degree (AEP) if it yields the first  $p$  coefficients exactly. The zeroth-order coefficient is reproduced by a local approximation, i.e., TF theory. A powerful feature of such asymptotic expansions is that they yield very accurate results even for small  $N$ , if the first few coefficients are known.

PFAs beyond the simple TF approximation have been derived [14,15] for a class of simple model systems in one dimension. In Sec. V we exemplify the accuracy of PFAs by calculating the expansion of the total energy in the large- $N$  limit for a generic, smooth one-body potential. Another limit in which TF theory becomes exact is the classical continuum limit, which we introduced as a device to derive the leading corrections to the TF density approximation [15]. We also assess the accuracy of existing PFAs in the classical continuum limit. In the course of this analysis we point out another difficulty with DFT that is not present in PFT. Functional construction in DFT is based on approximations to the XC energy. However, this causes an intrinsic ambiguity in the energy density, because any term whose integral over space vanishes—such as  $\Delta f(n(\mathbf{r}))$ —might be hidden in its definition [23]. This issue has been coined as the “gauge” ambiguity in energy densities for density functionals [24–26]. In PFT the energy densities are approximated directly. Therefore such an intrinsic ambiguity does not exist for potential functionals. Consequently, PFAs can be compared pointwise in space to evaluate their accuracy. We illustrate this with our kinetic energy PFA [13] by calculating bulk and surface energies for a simple case.

We contrast the direct and variational method of calculating the total energy in PFT for a simple model system in Sec. VI. We assess under what conditions the direct evaluation suffices and, thereby, examine the symmetry condition on the density-density response function for existing PFAs. The outcome of this analysis is a PFA to the density-density response function for noninteracting, spinless fermions in an arbitrary one-dimensional, smooth potential in a box.

In the Appendixes we show that the direct and variational evaluations of potential functional TF theory are equivalent. We also show what happens as box boundaries, needed in some formal constructions, are taken far away.

## II. EXACT STATEMENTS

In this section, we compare and contrast PFT and DFT; this section deals with the exact theory.

### A. Basic definitions

Begin with the variational principle in quantum mechanics by minimizing over  $N$ -particle wave functions  $\Psi$  that are antisymmetric, are normalized, and have finite kinetic energy:

$$E[v] = \min_{\Psi} (\langle \Psi | \hat{T} + \hat{V}_{ee} + \hat{V}_v | \Psi \rangle), \quad (1)$$

where  $\hat{T}$  is the kinetic energy operator,  $\hat{V}_{ee}$  the electron-electron repulsion, and  $\hat{V}_v$  an external one-body potential, explicitly denoting the potential as a subscript.

The heart of DFT is the HK theorem [18] which states, among other things, that the ground-state energy of an interacting electronic system can be found from

$$E[v] = \min_n \left\{ \tilde{F}[n] + \int d^3r n(\mathbf{r})v(\mathbf{r}) \right\}, \quad (2)$$

where  $\tilde{F}[n]$  is a universal functional of the one-electron density  $n(\mathbf{r})$ , because it is independent of  $v(\mathbf{r})$ . (We use a tilde to denote density functionals.) A useful way to define  $\tilde{F}[n]$  is via the constrained search procedure of Levy [16,27] and Lieb [17,28]:

$$\tilde{F}[n] = \min_{\Psi \rightarrow n} \langle \Psi | \hat{T} + \hat{V}_{ee} | \Psi \rangle, \quad (3)$$

which follows from Eq. (1) by writing the minimization in a two-step procedure, where the search is performed over all  $\Psi$ , yielding the density  $n(\mathbf{r})$ . The original work [18] was limited to nondegenerate ground states and assumed that most reasonable densities would be ground-state densities of some interacting electronic problem. The constrained search approach is a natural way around these difficulties.

But consider instead [11]

$$F[v] = \langle \Psi[v] | \hat{T} + \hat{V}_{ee} | \Psi[v] \rangle, \quad (4)$$

where  $\Psi[v]$  is the ground-state wave function of potential  $v(\mathbf{r})$ . Clearly,  $\Psi$  is independent of any constant in the potential, and all potential functionals are functions of the particle number  $N$  (for ease of notation, we do not denote this explicitly). We define it only for those potentials on which we wish to do quantum mechanics; a practical choice is the Hilbert space  $L^{3/2} + L^\infty$ , where we have a well-defined ground-state wave function and energy [29]. If, in addition, we denote the ground-state density as a functional of the potential,  $n[v](\mathbf{r})$ , and the dual density functional,  $\tilde{v}[n](\mathbf{r})$ , then

$$\tilde{F}[n] = F[\tilde{v}[n]], \quad F[v] = \tilde{F}[n[v]]. \quad (5)$$

In PFT, we can evaluate the ground-state energy directly,

$$E[v] = F[v] + \int d^3r n[v](\mathbf{r})v(\mathbf{r}), \quad (6)$$

or we can derive a variational principle in PFT by minimizing the expectation value of the total energy over trial potentials

$v'$ ,

$$E[v] = \min_{v'} (\langle \Psi[v'] | \hat{T} + \hat{V}_{\text{ee}} + \hat{V}_v | \Psi[v'] \rangle). \quad (7)$$

With the universal potential functional [11] defined in Eq. (4), we obtain

$$E[v] = \min_{v'} \left\{ F[v'] + \int d^3r n[v'](\mathbf{r}) v(\mathbf{r}) \right\}, \quad (8)$$

where in the exact case the minimizing trial potential is the true external potential  $v(\mathbf{r})$ . Because the right-hand functional is minimized, stationarity requires that the functional derivative vanish, i.e.,

$$\frac{\delta F[v]}{\delta v(\mathbf{r})} = - \int d^3r' v(\mathbf{r}') \chi[v](\mathbf{r}', \mathbf{r}), \quad (9)$$

where  $\chi(\mathbf{r}, \mathbf{r}') = \delta n[v](\mathbf{r}) / \delta v(\mathbf{r}')$  is the density-density response function. This is an important exact relation between  $F[v]$  and  $n[v](\mathbf{r})$ . Unfortunately, the relation is between functional derivatives, not the functionals themselves.

However, we can functionally integrate in several ways. The simplest is to use a coupling constant in the one-body potential:

$$v^\lambda[v](\mathbf{r}) = (1 - \lambda) v_0(\mathbf{r}) + \lambda v(\mathbf{r}), \quad (10)$$

where  $0 \leq \lambda \leq 1$ , and  $v_0(\mathbf{r})$  is some reference potential. Employing the integral form of the Hellmann-Feynman theorem, we obtain

$$E[v] = E_0 + \int_0^1 d\lambda \int d^3r n[v^\lambda[v]](\mathbf{r}) \Delta v(\mathbf{r}), \quad (11)$$

where  $\Delta v(\mathbf{r}) = v(\mathbf{r}) - v_0(\mathbf{r})$  is the difference between the true and the reference potential. Choosing a constant reference potential, here  $v_0(\mathbf{r}) = 0$ , the universal functional becomes

$$\mathcal{F}_n^{\text{cc}}[v] = \int d^3r \{ \bar{n}(\mathbf{r}) - n[v](\mathbf{r}) \} v(\mathbf{r}), \quad (12)$$

where  $\bar{n}(\mathbf{r}) = \int_0^1 d\lambda n[v^\lambda](\mathbf{r})$  denotes the average of the density over the coupling constant. We call  $\mathcal{F}^{\text{cc}}$  a *ffunctional* of  $n[w](\mathbf{r})$ , because it maps a functional (here  $n[w](\mathbf{r})$ , where  $w$  denotes a function of  $\mathbf{r}$ ) to another functional, the universal potential functional (see Appendix C for further discussion). The gist of Eq. (12) is that knowledge of the potential functional  $n[v](\mathbf{r})$  uniquely determines the universal functional  $\mathcal{F}^{\text{cc}}$  [13].

The exercise of checking that  $\mathcal{F}^{\text{cc}}$  as constructed by Eq. (12) satisfies Eq. (9) will prove useful. We take the functional derivative of Eq. (12) with respect to the potential  $v(\mathbf{r})$ . This yields

$$\begin{aligned} \frac{\delta \mathcal{F}^{\text{cc}}}{\delta v(\mathbf{r})} &= -n[v](\mathbf{r}) - \int d^3r' v(\mathbf{r}') \chi[v](\mathbf{r}', \mathbf{r}) \\ &+ \int_0^1 d\lambda \int d^3r' \chi[v^\lambda[v]](\mathbf{r}', \mathbf{r}) \frac{dv^\lambda[v](\mathbf{r}')}{d\lambda} \\ &+ \int_0^1 d\lambda \int d^3r' n[v^\lambda[v]](\mathbf{r}') \frac{d}{d\lambda} \frac{\delta v^\lambda[v](\mathbf{r}')}{\delta v(\mathbf{r})}, \end{aligned} \quad (13)$$

which satisfies Eq. (9) if, and only if,

$$\begin{aligned} n[v](\mathbf{r}) &= \int_0^1 d\lambda \int d^3r' \left\{ \chi[v^\lambda[v]](\mathbf{r}', \mathbf{r}) \frac{dv^\lambda[v](\mathbf{r}')}{d\lambda} \right. \\ &\left. + n[v^\lambda[v]](\mathbf{r}') \frac{d}{d\lambda} \frac{\delta v^\lambda[v](\mathbf{r}')}{\delta v(\mathbf{r})} \right\}. \end{aligned} \quad (14)$$

This condition is true, in turn [13], if, and only if, the density-density response function is symmetric under exchange of coordinates:

$$\chi[v](\mathbf{r}, \mathbf{r}') = \chi[v](\mathbf{r}', \mathbf{r}), \quad (15)$$

which is an important condition on  $n[v](\mathbf{r})$  and is satisfied by the exact density-density response function, by virtue of its being a second derivative of the ground-state energy.

## B. The dual of the Lieb functional

A more general form of the universal density functional was constructed by Lieb [17] using the Legendre transform of the energy. Its domain was extended to include any nonnegative densities that integrate to a given particle number and is a bifunctional of a potential and a density. This bifunctional is *not* used in PFT, and in fact, the entire procedure is unnecessary in PFT, because a detour via a density-potential mapping is unneeded. However, we show here its dual in PFT, to illustrate the differences between potential and density functionals and to make clear the distinction from the Lieb construction.

Lieb begins by defining a bifunctional of any pair  $n$  and  $v$ :

$$L[n, v] = E[v] - \int d^3r n(\mathbf{r}) v(\mathbf{r}). \quad (16)$$

Lieb's density functional is then defined as [17,30]

$$\tilde{F}_L[n] = \sup_v L[n, v]. \quad (17)$$

How is this related to the potential functional definition of the universal functional? Define the PFT dual of  $L[n, v]$ :

$$\tilde{L}[n_1, v_2] = \tilde{E}[n_1] - \int d^3r n[v_2](\mathbf{r}) \tilde{v}[n_1](\mathbf{r}), \quad (18)$$

where  $\tilde{v}[n](\mathbf{r})$  denotes the ground-state potential as a functional of  $n(\mathbf{r})$ . Starting from the variational principle, we find

$$\langle \Psi[v_2] | \hat{T} + \hat{V}_{\text{ee}} + \hat{V}_{v_1} | \Psi[v_2] \rangle \geq E[n_1], \quad (19)$$

leading to

$$F[v] = \sup_n \tilde{L}[n, v], \quad (20)$$

because in the exact theory  $F[v] = \mathcal{F}_n^{\text{cc}}[v]$ . This is the complement to Lieb's definition of the universal density functional in the context of PFT, but the much simpler definition of Eq. (4) suffices.

We note that there is another functional formulation of the electronic structure problem that was worked out by Englert [10], where the total energy is considered as a functional of the effective one-body potential  $v_{\text{eff}}(\mathbf{r})$ , density, and (negative) chemical potential  $\zeta$  simultaneously; i.e.,

$$\begin{aligned} \tilde{E}[v_{\text{eff}}, n, \zeta] &= \tilde{E}_1 + V_{\text{ee}}[n] - \zeta N \\ &- \int d^3r' n(\mathbf{r}') [v_{\text{eff}}(\mathbf{r}') - v(\mathbf{r}')], \end{aligned} \quad (21)$$

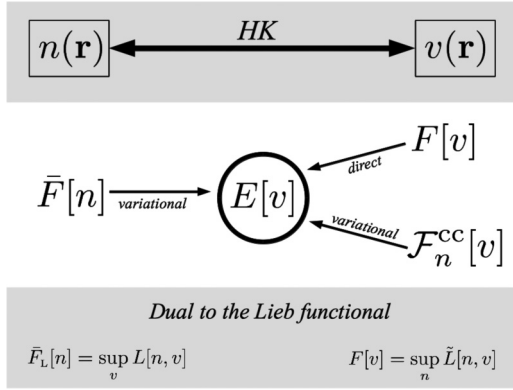


FIG. 1. Illustration of the relation between the universal functionals in DFT (left) and PFT (right).

where  $\bar{E}_1 = T[n] + \int d^3r' n(\mathbf{r}') [v_{\text{eff}}(\mathbf{r}') + \zeta]$ . This is different from either Lieb's density functional in Eq. (20) or the potential functionals defined in Eqs. (4) and (8). For example, within TF theory it can be shown that Eq. (21) yields the ground-state energy as the absolute maximum when a search over  $v_{\text{eff}}$  and  $\zeta$  is performed [31]. However, this only appears to be a contradiction with our formulation in Eq. (8), where the ground-state energy is the minimum of a search over trial potentials. Indeed this is consistent with both Lieb's formulation and our approach. Simply speaking, this formal difference from Englert's work originates from the explicit inclusion of the dependence on the particle number  $N$  in the total energy functional, in contrast to our definition.

To summarize this introduction to the exact theory, we illustrate the relation between DFT and PFT in Fig. 1. At the left we depict how the ground-state energy for the potential  $v$  is determined in DFT via  $\tilde{F}[n]$  by minimizing over trial densities. In PFT, on the other hand, the ground-state energy is found either directly, with the given functionals  $F[v]$  and  $n[v]$  via Eq. (6), or variationally, by sole knowledge of  $n[v]$  via  $\mathcal{F}_n^{\text{cc}}[v]$ .

### C. Noninteracting systems

Consider a system of fermions in some external potential  $v(\mathbf{r})$  which do *not* interact with one another. We use the subscript  $s$  to denote quantities and functionals for such a system, and  $F[v]$  reduces to  $T_S[v]$ . The variational principle simplifies to

$$E[v] = \min_{v'} \left\{ T_S[v'] + \int d^3r n_S[v'](\mathbf{r}) v(\mathbf{r}) \right\}, \quad (22)$$

and the coupling-constant expression is

$$T_{S,n_S}^{\text{cc}}[v] = \int d^3r \{ \bar{n}_S(\mathbf{r}) - n_S[v](\mathbf{r}) \} v(\mathbf{r}). \quad (23)$$

The consequence of Eq. (23) is that only the knowledge of the noninteracting density,  $n_S[v]$ , is required to determine the noninteracting kinetic energy  $T_S$ .

An alternative expression is given in terms of the virial theorem for the noninteracting kinetic energy [32]:

$$\nabla^2 t_S(\mathbf{r}) = -\frac{d}{2} \nabla \{ n(\mathbf{r}) \nabla v_S(\mathbf{r}) \}, \quad (24)$$

where  $d$  is the dimensionality of space and  $t_S(\mathbf{r})$  the kinetic energy density, such that  $T_S = \int d^3r t_S(\mathbf{r})$ .

### D. Kohn-Sham scheme

So far we have discussed the potential functional analog of HK-type DFT, where knowledge of the density suffices to determine the total energy of either an interacting or a noninteracting system by evaluation of the corresponding potential functionals, such as the universal functional and the functional for the noninteracting kinetic energy on the density.

But also the noninteracting case can be utilized to yield the total energy of an interacting system of electrons. This is achieved via the celebrated KS scheme. In what follows we describe how PFT could be employed in the KS construct. The interacting system is mapped onto a noninteracting system, requiring that both have the same density. This mapping is achieved by the KS potential,

$$v_S(\mathbf{r}) = v(\mathbf{r}) + \tilde{v}_H[n_S[v_S]](\mathbf{r}) + \tilde{v}_{\text{XC}}[n_S[v_S]](\mathbf{r}), \quad (25)$$

mimicking all many-body interactions among the electrons in the usual KS-DFT sense via the Hartree and XC potentials:

$$\tilde{v}_H[n](\mathbf{r}) = \frac{\delta \tilde{U}[n]}{\delta n(\mathbf{r})} = \int d^3r' \frac{n(\mathbf{r}')}{|\mathbf{r} - \mathbf{r}'|}, \quad (26)$$

$$\tilde{v}_{\text{XC}}[n](\mathbf{r}) = \delta \tilde{E}_{\text{XC}}[n] / \delta n(\mathbf{r}). \quad (27)$$

With a potential functional to the noninteracting density  $n_S[v_S](\mathbf{r})$ , which is identical to the interacting density  $n(\mathbf{r})$  for the exact KS potential  $v_S(\mathbf{r})$ , Eq. (25) can be solved by standard iteration techniques, *bypassing* the need to solve the KS equations. The process of a KS-PFT calculation is illustrated in Fig. 2. A given  $n_S[v_S]$  eliminates the need to solve any differential equation in each iteration.

At the end of this iterative process we determine the total energy of the interacting electronic system via

$$E[v] = T_{S,n_S}^{\text{cc}}[v_S] + \tilde{U}[n_S[v_S]] + \tilde{E}_{\text{XC}}[n_S[v_S]] + \int d^3r n_S[v_S] v(\mathbf{r}). \quad (28)$$

Both the Hartree and the XC contribution can be evaluated readily for a given  $n_S[v_S](\mathbf{r})$ . The only missing ingredient for evaluation of Eq. (28) is the noninteracting kinetic energy. But we can use our result from the previous section. The noninteracting kinetic energy of the KS electrons is given via Eq. (23), where in that expression the external potential  $v(\mathbf{r})$  becomes the KS potential  $v_S(\mathbf{r})$ ; i.e.,

$$T_{S,n_S}^{\text{cc}}[v] = \int d^3r \{ \bar{n}_S(\mathbf{r}) - n_S[v_S](\mathbf{r}) \} v_S(\mathbf{r}). \quad (29)$$

The knowledge of  $n_S[v_S](\mathbf{r})$ , which produces the corresponding  $v_S(\mathbf{r})$  self-consistently, suffices to determine the noninteracting kinetic energy of the KS system.

### III. APPROXIMATIONS

In practice, the HK type of DFT requires an approximation to the universal functional,  $\tilde{F}^A[n]$ , where the superscript  $A$  denotes an approximation such as that used in TF theory, as discussed in the next section. Via the variational principle we

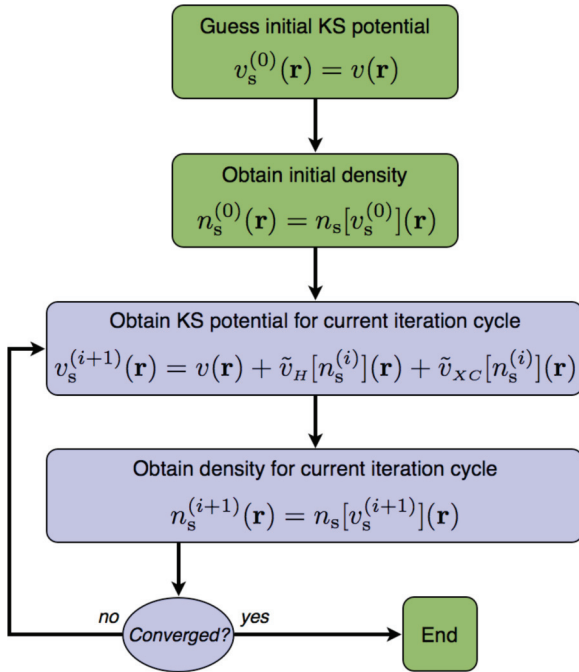


FIG. 2. (Color online) Self-consistent cycle in a PFT calculation within the KS scheme: In contrast to a KS calculation in DFT, here, in PFT, there is no need to solve the KS equations. The iteration begins by guessing a KS potential and obtaining the initial density via  $n_s^{(0)}(\mathbf{r}) = n_s[v_s^{(0)}](\mathbf{r})$ . Evaluating Eq. (25) on the initial density,  $n_s^{(0)}(\mathbf{r})$ , yields the KS potential of the next iteration,  $v_s^{(1)}(\mathbf{r})$ . The corresponding density is obtained by  $n_s^{(1)}(\mathbf{r}) = n_s[v_s^{(1)}](\mathbf{r})$ , which is needed to compute the KS potential of the next iteration. This process is continued until convergence is achieved.

then obtain a relation that determines the density for a given  $v(\mathbf{r})$ :

$$\frac{\delta}{\delta n(\mathbf{r})} \left( \tilde{F}^A[n] + \int d^3r \{v(\mathbf{r}) - \mu\} n(\mathbf{r}) \right) = 0, \quad (30)$$

where the Lagrange multiplier  $\mu$  is identical to the chemical potential. This yields an integrodifferential equation in  $n(\mathbf{r})$  which is typically solved self-consistently, producing  $n^A(\mathbf{r})$ , whose details depend on the choice of the approximation  $\tilde{F}^A[n]$ .

On the other hand, PFT works in a very different way. In the most general case, we have an approximation to the pair  $\{n[v](\mathbf{r}), F[v]\}$  to obtain the total energy of the many-body quantum system directly via Eq. (6); in the direct evaluation we need a PFA to both the density and the universal functional as a functional of the external one-body potential. This was the approach used in Refs. [14,15], but it does not take advantage of the exact conditions derived in Ref. [13]. The semiclassical approach developed in those works [14,15] yields more accurate densities than kinetic energies, due to the need to take two spatial derivatives to calculate the kinetic energy and, furthermore, is much easier for densities than kinetic energies, because expansions need only be performed to a lower order [15].

To take advantage of the results in the previous section, we now discuss their logic when applied to approximate calculations. If a pair of approximations  $\{F^A, n^A\}$  satisfies

Eq. (9) at  $v(\mathbf{r})$ , then Eqs. (6) and (8) yield identical results. Then no minimization procedure is needed. But this is *not* guaranteed *a priori* in approximate PFT. Thus, there seem to be two obvious disadvantages of PFT. First, we need to approximate the density and the universal functional separately. Second, to take advantage of Eq. (8), we need to know whether a given pair  $\{n^A[v](\mathbf{r}), F^A[v]\}$  satisfies the variational principle.

The functional integration in terms of the coupling constant [13] removes one of these problems. With a PFA to the density,  $n^A[v](\mathbf{r})$ , the conjugate approximation for the universal functional follows from Eq. (12) and reads

$$\mathcal{F}_{n^A}^{\text{cc}}[v] = \int d^3r \{ \tilde{n}^A(\mathbf{r}) - n^A[v](\mathbf{r}) \} v(\mathbf{r}). \quad (31)$$

The important point to note is that only one approximation, namely,  $n^A[v](\mathbf{r})$ , is required to uniquely determine an approximation to the universal functional. As a result, we obtain the reverse of the common procedure in DFT: In variational PFT we *first* specify which PFA we use for  $n^A[v](\mathbf{r})$ , which *then* determines the corresponding  $F^A[v]$  via Eq. (31).

But this does not automatically cure the second problem. An approximate pair constructed in this way does *not* automatically satisfy the variational principle. It is not even clear which method of calculation (direct or by use of the variational principle) would yield a more accurate answer for a given PFA to the density. However, the previous section shows that a sufficient condition is the symmetry condition in Eq. (15), which guarantees identical results, eliminating the need to perform the minimization.

The utility of this approach for calculations on interacting systems is probably limited in practice, for the same reason that TF theory is largely abandoned in favor of the KS scheme. Pure PFT requires a sufficiently accurate approximation to the density of *interacting* electrons as a functional of the external one-body potential, to produce approximate energetics that are accurate enough to bind molecules and generally compete for accuracy with KS calculations using the present XC approximations.

A much more likely application of these results is for noninteracting electrons in a KS potential. All previous general statements for the interacting case analogously apply to the noninteracting case. First, recall the standard procedure in KS-DFT: The XC energy is approximated, and the KS equations are solved self-consistently. In KS-PFT, however, we additionally need a PFA to the noninteracting density, which is a less complicated object to approximate than its interacting counterpart. Then the self-consistent cycle, shown in Fig. 2, is solved; any existing density functional approximation to the XC energy can be employed in Eq. (25). The total energy of the many-body quantum system is finally extracted from Eq. (28), where the noninteracting kinetic energy of KS electrons is calculated via the conjugate approximation to Eq. (23):

$$\mathcal{T}_{S, n_S^A}^{\text{cc}}[v] = \int d^3r \{ \tilde{n}_S^A(\mathbf{r}) - n_S^A[v](\mathbf{r}) \} v_S[v](\mathbf{r}). \quad (32)$$

Note that the only approximation needed to perform this self-consistent KS-PFT calculation is  $n_S^A[v](\mathbf{r})$  (besides the approximation to  $E_{\text{XC}}$ , which is also required in KS-DFT); this scheme is more efficient by several orders of magnitude than a standard KS-DFT calculation, because the KS equations

never have to be solved. However, the applicability of KS-PFT crucially depends on the accuracy of  $n_S^A[v](\mathbf{r})$ ; a major fraction of the total energy is kinetic, such that only tiny errors are allowed. Nevertheless, highly accurate approximations to  $n_S^A[v](\mathbf{r})$  that satisfy this restriction have already been derived for model systems [14,15], and approximations for more realistic external potentials are in development [33,34].

#### IV. THOMAS-FERMI THEORY: AN ILLUSTRATION

In this section we show how PFAs work. We use TF theory for this illustration, because its simplicity in treating the electron-electron interaction makes the presentation explicit. First, we recall the usual density functional formulation of TF theory for interacting electrons. Then we formulate its potential functional counterpart and confirm that both approaches yield the same result.

##### A. Density functional approximation

In the density functional formulation, we need simply an approximation to  $F[n]$ , which, in TF theory, is

$$\tilde{F}^{\text{TF}}[n] = \tilde{T}_S^{\text{TF}}[n] + \tilde{U}[n], \quad (33)$$

which is the sum of the local approximation for the kinetic energy of a noninteracting uniform gas,

$$\tilde{T}_S^{\text{TF}}[n] = \frac{3}{10} (3\pi^2)^{2/3} \int d^3r n(\mathbf{r})^{5/3}, \quad (34)$$

and the Hartree energy,

$$\tilde{U}[n] = \frac{1}{2} \int d^3r n(\mathbf{r}) \tilde{v}_H[n](\mathbf{r}), \quad (35)$$

where

$$\tilde{v}_H[n](\mathbf{r}) = \frac{\delta U}{\delta n(\mathbf{r})} = \int d^3r' \frac{n(\mathbf{r}')}{|\mathbf{r} - \mathbf{r}'|}. \quad (36)$$

This yields the TF energy functional:

$$E^{\text{TF}}[v] = \min_n \left\{ \tilde{F}^{\text{TF}}[n] + \int d^3r n(\mathbf{r}) v(\mathbf{r}) \right\}. \quad (37)$$

To find the minimizing density, we functionally differentiate, yielding a Euler equation for the self-consistent TF density:

$$n^{\text{TF}}(\mathbf{r}) = \frac{1}{3\pi^2} \{2[\mu - v(\mathbf{r}) - \tilde{v}_H[n^{\text{TF}}](\mathbf{r})]\}^{3/2}. \quad (38)$$

The density is taken to vanish whenever the argument on the right is negative, and the chemical potential chosen via normalization,

$$\int d^3r n^{\text{TF}}(\mathbf{r}) = N. \quad (39)$$

Finally, we note that this can always be interpreted in terms of the KS scheme. The TF theory ignores XC contributions, so that

$$\tilde{v}_S^{\text{TF}}[n](\mathbf{r}) = v(\mathbf{r}) + \tilde{v}_H[n](\mathbf{r}), \quad (40)$$

and the density satisfies

$$n^{\text{TF}}(\mathbf{r}) = \frac{1}{3\pi} \{2\{\mu - \tilde{v}_S^{\text{TF}}[n^{\text{TF}}](\mathbf{r})\}\}^{3/2}. \quad (41)$$

##### B. Potential functional approximations

We now show how TF theory can be derived as a PFA. Although the final equations are identical, their derivation is very different.

Because interaction effects are less explicit in PFT, we begin with an analysis of the noninteracting case. All PFAs start with the density as a functional of the potential. For plane waves of an extended system with constant potential  $v$ , one finds

$$n_S(v) = \frac{1}{3\pi^2} [2(\mu - v)]^{3/2}. \quad (42)$$

This then leads to the TF approximation in PFT for noninteracting electrons in  $v(\mathbf{r})$ :

$$n_S^{\text{TF}}[v](\mathbf{r}) = \frac{1}{3\pi^2} \{2[\mu - v(\mathbf{r})]\}^{3/2}. \quad (43)$$

The same plane waves yield a kinetic energy density in the box,

$$t_S(v) = \frac{1}{10\pi^2} [2(\mu - v)]^{5/2}, \quad (44)$$

which produces the TF PFT for  $T_S$ :

$$T_S^{\text{TF}}[v] = \frac{1}{10\pi^2} \int d^3r \{2[\mu - v(\mathbf{r})]\}^{5/2}. \quad (45)$$

In fact, insertion of Eq. (43) into Eq. (45), eliminating  $v(\mathbf{r})$ , produces the usual TF DFT [29]. Thus the duality shows that knowledge of the density functionals produces the corresponding potential functionals, and vice versa:

$$T_S^{\text{TF}}[v] = \tilde{T}_S^{\text{TF}}[n_S[v]], \quad \tilde{T}_S^{\text{TF}}[n_S] = T_S^{\text{TF}}[\tilde{v}[n_S]]. \quad (46)$$

Armed with this pair of approximations, we can perform either a direct evaluation,

$$E_{\text{dir}}^{\text{TF}}[v] = T_S^{\text{TF}}[v] + \int d^3r n_S^{\text{TF}}[v](\mathbf{r}) v(\mathbf{r}), \quad (47)$$

or a minimization,

$$E_{\text{var}}^{\text{TF}}[v] = \min_{v'} \left\{ T_S^{\text{TF}}[v'] + \int d^3r n_S^{\text{TF}}[v'](\mathbf{r}) v(\mathbf{r}) \right\}; \quad (48)$$

and we do not know *a priori* if these yield the same result. In Appendix A we show that for TF theory, in fact, Eqs. (47) and (48) are equivalent.

Alternatively, we can use our density PFA to *construct* a kinetic energy functional via Eq. (23). Applying this leads to

$$T_{S,n_S^{\text{TF}}}^{\text{cc}}[v] = \int d^3r \{ \tilde{n}_S^{\text{TF}}(\mathbf{r}) - n_S^{\text{TF}}[v](\mathbf{r}) \} v(\mathbf{r}), \quad (49)$$

which is identical to  $T_S^{\text{TF}}[v]$ . This can be shown in the following way: Begin with Eq. (47) and show that it yields the same energy when Eq. (49) is used; i.e., we want to show the equality

$$E_{\text{dir}}^{\text{TF}}[v] = T_{S,n_S^{\text{TF}}}^{\text{cc}}[v] + \int d^3r n_S^{\text{TF}}[v](\mathbf{r}) v(\mathbf{r}). \quad (50)$$

Introducing a coupling constant as in Eq. (10) [with  $v_0(\mathbf{r}) = 0$ ], we can write

$$E_{\text{dir}}^{\text{TF}}[v] = \int_0^1 d\lambda \frac{dE_{\text{dir}}^{\text{TF}}[v^\lambda[v]]}{d\lambda}. \quad (51)$$

We further take advantage of the fact that the Hellmann-Feynman theorem is satisfied in TF theory [35], yielding

$$\frac{dE_{\text{dir}}^{\text{TF}}[v^\lambda[v]]}{d\lambda} = \int d^3r n_S^{\text{TF}}[v^\lambda[v]](\mathbf{r})v(\mathbf{r}). \quad (52)$$

Inserting this into Eq. (51) yields the equality in Eq. (50) via the definition in Eq. (49) and proves the equivalence of  $\mathcal{T}_{S,n_S^{\text{TF}}}^{\text{cc}}[v]$  and  $T_S^{\text{TF}}[v]$ . Thus, from our general proof, we know that iff our density PFA satisfies the symmetry condition in Eq. (15), then direct evaluation yields the same result that minimization does, so that we can dispense with minimization. In Sec. VI, we prove just that in one dimension, but the proof is trivial to generalize to three.

From a different perspective, if we did not know  $T_S^{\text{TF}}[v]$ , our coupling-constant procedure *generates* the correct formula.

But full TF theory is about interacting particles, and uses the Hartree approximation to treat the interaction. To generate this in PFT, write the interacting density in terms of the KS potential,

$$n^{\text{TF}}[v](\mathbf{r}) = \frac{1}{3\pi} (2\{\mu - v_S[v](\mathbf{r})\})^{3/2}, \quad (53)$$

and write the Poisson equation in reverse,

$$n^{\text{TF}}[v](\mathbf{r}) = -\frac{1}{4\pi} \nabla^2 v_H[v](\mathbf{r}), \quad (54)$$

where

$$v_S[v](\mathbf{r}) = v(\mathbf{r}) + v_H[v](\mathbf{r}). \quad (55)$$

Together, Eqs. (53) and (54) produce the implicit  $v$  dependence of  $v_H(\mathbf{r})$  and, so, define the TF PFA for the density of interacting electrons. In fact, use of the equation for the potential is how TF equations are usually solved for atoms [36–38]. In practice, we solve Eq. (55) as illustrated in Fig. 2. The iteration starts by setting  $v_H(\mathbf{r}) = 0$  in Eq. (55), evaluating  $n_S^{\text{TF}}[v](\mathbf{r})$  via Eq. (53), and finding the resulting  $v_H[v](\mathbf{r})$  in Eq. (54), which is then used to determine the KS potential of the next iteration cycle via Eq. (55), yielding the corresponding density via Eq. (53), which, inserted into the left-hand side of Eq. (54), yields the Hartree potential for the following iteration. This process is continued until convergence. Finally, the converged KS potential and density are found.

Then we apply our coupling-constant trick and use as the kinetic energy functional the TF analog of Eq. (32); i.e.,

$$T_{S,n_S^{\text{TF}}}^{\text{cc}}[v] = \int d^3r \{ \bar{n}_S^{\text{TF}}(\mathbf{r}) - n_S^{\text{TF}}[v](\mathbf{r}) \} v_S[v](\mathbf{r}). \quad (56)$$

This is almost identical to Eq. (49), with the only difference that  $v(\mathbf{r})$  is replaced by  $v_S[v](\mathbf{r})$ , which is determined self-consistently as just described. This leads to the following PFA to the universal functional:

$$\mathcal{F}_{n_S^{\text{TF}}}^{\text{cc}}[v] = T_{S,n_S^{\text{TF}}}^{\text{cc}}[v] + U[v], \quad (57)$$

which is equivalent to  $F^{\text{TF}}[v]$ . Again, we can check duality:

$$U[v] = \tilde{U}[n^{\text{TF}}[v]], \quad \tilde{U}[n] = U[\tilde{v}^{\text{TF}}[n]]. \quad (58)$$

Given its symmetry, it does not disturb the symmetry condition, so that direct evaluation remains sufficient, even in the interacting case.

## V. ASYMPTOTIC ANALYSIS

In this section we apply the theory of the previous sections to recent suggestions for PFAs. We restrict the following discussion to noninteracting, spinless fermions in a one-dimensional, smooth potential with box boundaries, because for this class of potentials an accurate PFA to the density has already been derived [14,15] and is of convenient analytical form. The derivation produced  $n_S^{\text{sc}}[v](x) = n_S^{\text{sm}}[v](x) + n_S^{\text{osc}}[v](x)$ , where the first term is a smooth, TF-like piece and the second an oscillating, quantum correction, which are defined as

$$n_S^{\text{sm}}[v](x) = \frac{k}{\pi}, \quad (59)$$

$$n_S^{\text{osc}}[v](x) = -\frac{\sin 2\theta}{2\tau_L k \sin \alpha}, \quad (60)$$

where we drop the dependency on  $x$  to preserve a concise notation. The quantities in Eq. (59) are the Fermi wave vector

$$k = \sqrt{2[\epsilon_F - v(x)]}, \quad (61)$$

the classical phase

$$\theta = \int_0^x dx' p, \quad (62)$$

where  $p = \sqrt{2(\epsilon_F - v(x'))}$ , and the classical time for a particle with energy  $\epsilon_F$  to travel from 0 to  $x$  or  $L$ ,

$$\tau = \int_0^x dx'/p, \quad \tau_L = \int_0^L dx/k, \quad (63)$$

and the abbreviation  $\alpha = \pi\tau/\tau_L$ . Note that all quantities in Eq. (59) are evaluated at the Fermi energy  $\epsilon_F$ .

In Ref. [13] we demonstrated that, for generic external potentials which are sufficiently smooth (such that the basic assumption of the WKB approximation is valid), our coupling-constant method combined with the semiclassical density PFA (derived in Ref. [14]) yields highly accurate total energies, almost indistinguishable from the exact answer already for any  $N \geq 2$ . In the following we analyze the accuracy of those PFAs, both in terms of energy and in real space. Then we explain the source of the observed accuracy via an asymptotic analysis in the large- $N$  and the classical continuum limit [15]. Furthermore, we calculate the contributions to the asymptotic correctness coming from distinct regions—the interior and the edge; these are analogs of the surface and the bulk of a real solid. In the following we present only the essence of our analysis. We refer the interested reader to the Supplemental Material [39] for further numerical details.

### A. Large- $N$ asymptotic expansion of energies

We analyze the asymptotic behavior of the total energy in the large- $N$  limit to assess the accuracy of approximations. We examine the behavior of two PFAs: the independent semiclassical approximation (ISA) and the density-driven semiclassical approximation (DSA).

The first consists of two independent semiclassical approximations: one for the density, first derived in Ref. [14], and the other for the kinetic energy density. This derivation requires

TABLE I. Exact total energy and errors in the TF approximation, ISA, and DSA for  $N$  particles in the external potential  $v(x) = -8 \sin^2(\pi x)$ , where  $0 \leq x \leq 1$ .

$N$	$E$	$E^A - E$		
		TF	ISA	DSA
1	-1.1615	-1.603	-0.1825	-0.0221
2	14.510	-9.554	-0.1200	0.0054
4	129.95	-40.78	-0.0357	0.0011
8	972.65	-162.5	-0.0098	0.0002
16	7316.4	-642.8	-0.0026	$2 \times 10^{-5}$
24	24082	-1438	-0.0010	$7 \times 10^{-6}$

expansion to a higher order in  $\hbar$ , and yields an asymptotically correct expansion in the interior, but fails near an edge. This failure was patched to the asymptotically correct solution near the edge in Ref. [14], in order to produce a uniformly asymptotic approximation. A better patching scheme was developed in Ref. [15].

The second PFA, denoted the DSA, was first derived in Ref. [13], using the coupling-constant construction studied here. The advantage is that one needs only the semiclassical formula for the density alone, which is uniformly asymptotic, and so the kinetic energy density derived from it by functional integration via the coupling-constant method should automatically be uniformly asymptotic. An obvious question is its performance relative to the ISA, especially the behavior of both near the edge of the box.

In Table I, we list total energies for several  $N$  values for a generic external potential  $v(x) = -8 \sin^2 \pi x$ ,  $0 \leq x \leq 1$ . The incredibly rapid convergence of the DSA to the exact energy as  $N$  grows is readily apparent. We can understand and quantify this as follows: Expanding the total energy in powers of  $N$  yields

$$E(N)/N^3 = c_0 + c_1/N + c_2/N^2 + c_3/N^3 + c_4/N^4 + \dots \quad (64)$$

We characterize the accuracy of an approximation [14] by measuring the deviation from these exact coefficients. We perform this analysis explicitly for the generic external potential, assuming that the qualitative features are independent of the specific potential, once it is reasonably smooth. In Fig. 3, we plot  $E(N)/N^3$  both exactly and for the various approximations.

Because of the box boundary conditions, the energies approach those of a flat box as  $N$  grows, and in fact, the leading two coefficients are just  $c_0 = \pi^2/6$  and  $c_1 = \pi^2/4$ , respectively. Remarkably, the TF approximation is only AE0, i.e., it errs in the value of  $c_1$ , as it does *not* recover the flat box results exactly [14]. But the semiclassical corrections yield a great improvement over TF theory. To analyze them, we define the residual energy,  $\Delta E = E - E^{\text{flat}}$ , where the flat box result is known analytically. Then

$$\Delta E(N) = c'_2 N + c_3 + c_4/N + \dots, \quad (65)$$

where  $c'_2 = (c_2 - \pi^2/12)$ . We find that the ISA correctly reproduces  $c'_2 = -4$ , but makes a small error in  $c_3$  (about 0.25%). Thus this approximation is AE2, as discussed in Ref. [14], and is almost AE3.

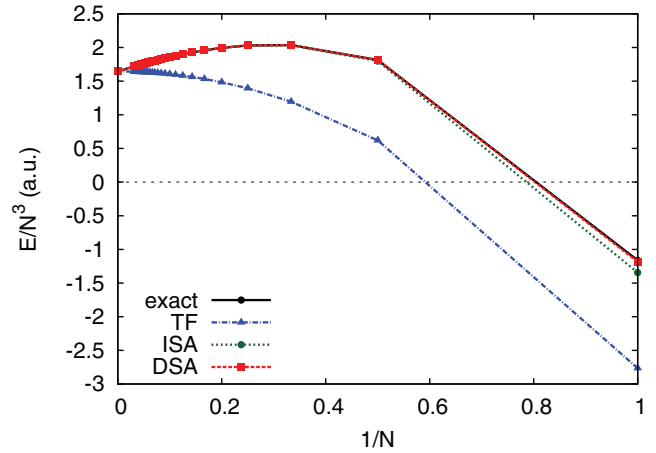


FIG. 3. (Color online) Numerical confirmation of the leading coefficient  $c_0$  of Eq. (64) from the exact calculation, ISA, and DSA for  $v(x) = -8 \sin^2(\pi x)$ , where the maximum number of particles considered is  $N = 32$ .

But the new approximation, the DSA, using only the density formula and coupling-constant integration, is at least AE4. It is beyond our numerical accuracy to determine  $c_5$  sufficiently accurately, although it appears that even this coefficient may be exact within the DSA. Thus, by reproducing two more terms in the asymptotic expansion exactly, we get tremendous improvements in accuracy, even at  $N = 1$ . This illustrates the potential of the coupling-constant method to generate incredibly accurate approximations.

### B. Classical continuum limit of energies

An alternative limit in which TF also becomes exact was described in Ref. [15]. We define the approach to the classical continuum limit by increasing the number of particles in a system from its original value  $N$  to  $N' > N$ , while simultaneously replacing  $\hbar$  with  $\gamma\hbar$ , where  $\gamma = N/N'$ . As  $N' \rightarrow \infty$ , the energy differences between discrete eigenvalues becomes infinitesimal and a continuum is formed. The advantage of this limit, as opposed to large  $N$ , is that it approaches the TF solution of the original problem with  $N$  particles, rather than approaching the  $N \rightarrow \infty$  problem of the previous section.

Expanding the total energy in powers of  $\gamma$  about 0 yields the expansion

$$E(\gamma) = E^{\text{TF}} (1 + b_1 \gamma + b_2 \gamma^2 + \dots), \quad (66)$$

where

$$b_p = \frac{1}{p!} \left. \frac{d^p E}{d\gamma^p} \right|_{\gamma=0} / E^{\text{TF}}. \quad (67)$$

Such an expansion is expected to be asymptotic rather than convergent. We also define  $E^{(p)}$  as the sum up to the  $p$ th order of such terms. We find, for  $N = 1$ , that while  $E^{(2)}$  is more accurate than lower order truncations,  $E^{(3)}$  overshoots. For  $N > 1$ , all successive terms up to third order always improve accuracy.

Under this  $\gamma$  scaling, the TF approximation is independent of  $\gamma$ . We find that both PFAs, the ISA and DSA, reproduce  $b_1$  exactly, but neither yields  $b_2$ . This is not surprising, as these approximations were derived only to yield the leading

corrections to TF in this limit. For  $N = 1$ , we find that neither approximation yields particularly accurate expansion coefficients and that their absolute errors for the coefficients are comparable. Regardless, these errors in the coefficients do not translate into an inaccurate energy; as we have shown in the previous section, the DSA energy is very accurate for  $N = 1$ . As  $N$  grows, the errors in the coefficients rapidly shrink, but from analysis of the coefficients alone, the DSA would appear to be no more accurate than the ISA. As shown in the previous section, however, the DSA is far more accurate and converges more rapidly than the ISA with increasing  $N$ . Therefore the asymptotic expansion in  $\gamma$  is not useful for understanding the improved accuracy of the DSA relative to the ISA.

### C. Analysis in real space

In density functional approximations, a difficult and vexing issue is the ambiguity of the energy density of an approximate density functional for an energy [24,25]. For example, one can always add the Laplacian of the density to the energy density of even a local approximation without changing the functional, since that addition integrates to 0 as long as the density vanishes on the boundary. This difficulty complicates any pointwise comparison between approximate functionals [40] and has hampered our ability to construct improved approximations, especially local hybrids [24,41].

A great advantage of PFT is that this ambiguity does not exist: PFAs approximate a given choice of exact energy density and, so, can be compared pointwise. There is no “gauge” ambiguity [26].

In Fig. 4, we illustrate this for a single particle in a single well of depth 8. The ISA approximates one definition of the kinetic energy density, while the DSA approximates another. But in each case, they can be compared for accuracy pointwise to the respective exact curve. Again, we see that the DSA is more accurate everywhere. Its maximum errors are much smaller than those of the ISA, and the average errors are also much smaller.

To check this idea, we have seen above that both semiclassical PFAs show higher order asymptotic exactness than

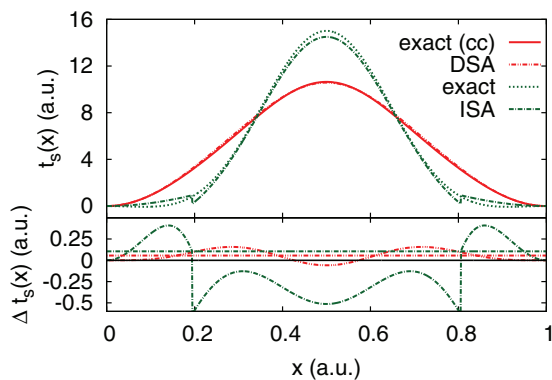


FIG. 4. (Color online) Comparison of the ISA kinetic energy density [lower dash-dotted (green) line] with its exact counterpart [lower dotted (green) line] and of the DSA kinetic energy density [upper dash-dotted (red) line] with its exact counterpart [solid (red) line] for one particle in  $v(x) = -8 \sin^2(\pi x)$ . The lower panel shows the errors, with average errors indicated by straight dash-dotted lines.

the TF approximation. We now ask if these improvements are visible in separate spatial regions, not just for quantities integrated over the entire system. In particular, we know that the limit as  $\gamma \rightarrow 0$  is different for fixed values of  $x$  (interior) than for fixed values of  $\gamma x$ , the edge (or surface) region [15]. But the semiclassical density approximation is supposed to be uniformly asymptotic, i.e., to have the same degree of AE for each region separately. To test this, we must define a dividing line between the interior and the edge. We choose the half-phase point  $x_{\pi/2}$ , defined by the following condition on the classical phase [14]:

$$\theta(x_{\pi/2}) = \pi/2. \quad (68)$$

This is our measure to split the box into an interior ( $L/2 - |L/2 - x| > x_{\pi/2}$ ) and edges (the rest).

This condition has been used for the boundary-layer analysis of the ISA in Ref. [15]. As  $N$  grows,  $x_{\pi/2} \sim 1/N$ ; or as  $\gamma \rightarrow 0$ ,  $x_{\pi/2} \sim \gamma$ . We define a surface kinetic energy as the energy in this region and analyze the accuracy of our approximations for this quantity.

The energy from distinct regions follows the same expansions as Eqs. (64) and (66), but with different coefficients  $c_p^{\text{int}}$ ,  $c_p^{\text{edge}}$ ,  $b_p^{\text{int}}$ , and  $b_p^{\text{edge}}$ . As  $N$  grows, the boundary between the edge and the interior—the half-phase point  $x_{\pi/2}$ —is shifted towards the edge, such that in the limit  $N \rightarrow \infty$  the edge region vanishes and the interior extends over the entire length of the system. The same is true for the classical continuum limit. Hence, the leading order coefficient of both expansions close to the edge vanishes; i.e.,  $c_0^{\text{edge}} = 0$  and  $b_0^{\text{edge}} = 0$ . Also, note that we need to distinguish between two exact results when splitting up the energy into contributions from different spatial regions. This is due to the fact that we use two different definitions of the kinetic energy density. The ISA stems from the Laplacian definition, whereas the DSA yields a different definition as illustrated in Fig. 4. However, the difference in the energy values between these definitions vanishes with increasing  $N$ ; therefore we report only exact regional energies using the Laplacian definition, but note that the errors of DSA are calculated with respect to the exact energy density defined by the coupling-constant method for each region. First, we consider the total energies of the interior given in the  $E$  columns in Table II. We plot  $E^{\text{int}}(N)/N^3$  in Fig. 5, illustrating the large- $N$  limit, in which the energy expansion in the interior approaches  $\pi^2/6$ . This analysis also yields that the ISA correctly reproduces  $c_0$ ,  $c_1^{\text{int}} = 1.313$ , and  $c_2^{\text{int}} = -4.492$  but fails to yield  $c_3^{\text{int}}$  (with the small error of about 0.1%). On the other hand, the DSA exactly reproduces the coefficients up to at least  $c_4^{\text{int}}$ .

Next we consider the edge region, for which the energy contributions and errors of approximations are listed in the TF, ISA, and DSA columns in Table II. As the size of this region vanishes in the limit  $N \rightarrow \infty$ , the leading term in the large- $N$  expansion falls off linearly with  $N$ . This is illustrated in Fig. 6. In analogy to the interior, the ISA correctly yields  $c_1^{\text{edge}} = 1.147$  and  $c_2^{\text{edge}} = 1.16$  but makes a mistake for  $c_3^{\text{edge}}$ , by about 0.5%. The DSA, however, yields exact coefficients up to at least  $c_4^{\text{edge}}$  and probably also for higher order contributions. The numerical accuracy of our analysis is not high enough to give a definite answer beyond this order.

TABLE II. Exact total energy and errors of approximations (TF, ISA, and DSA) in the interior and close to the edge for  $N$  particles in the external potential  $v(x) = -8 \sin^2(\pi x)$ , where  $0 \leq x \leq 1$ .

$N$	Interior				Edge			
	$E$	$E^A - E$			$E$	$E^A - E$		
		TF	ISA	DSA		TF	ISA	DSA
1	-0.6721	-1.081	-0.1051	0.0076	-0.4891	-0.5219	-0.0774	-0.0297
2	9.631	-8.215	-0.1505	0.0068	4.876	-1.3361	0.0304	-0.0014
4	108.5	-41.28	-0.0666	0.0012	21.41	0.5091	0.0308	$-6 \times 10^{-5}$
8	891.2	-178.9	-0.0199	0.0002	81.23	16.49	0.0101	$-1 \times 10^{-6}$
16	7004	-738.7	-0.0054	$2 \times 10^{-5}$	310.8	96.16	0.0028	$-2 \times 10^{-8}$
24	23 391	-1677	-0.0025	$7 \times 10^{-6}$	686.9	239.2	0.0013	$-3 \times 10^{-9}$

In conclusion, we could demonstrate that even when we consider energy contributions from separate spatial regions, the ISA is AE2, whereas the DSA is at least AE3. Furthermore, this analysis shows that the accuracy achieved by both approximations over the entire system is not due to error cancelations in different spatial regions; it is caused by virtue of both approximations capturing the large- $N$  asymptotic expansion in separate spatial regions sufficiently accurately.

## VI. THE IMPORTANCE OF BEING SYMMETRIC

In this section we contrast the direct method of calculating the total energy in PFT given by Eq. (6) with the variational method in Eq. (8). Determining the total energy variationally as in Eq. (8) is sensible only for calculations that involve approximations. In the exact case the total energy is always minimized by the true external potential of the given problem. We also demonstrate that the particular PFA to the density,  $n_S^A[v](x)$ , derived in Ref. [14], violates the symmetry condition of Eq. (15). Consequently, when we perform a search over trial potentials, the minimum energy is not given at  $v'(x) = v(x)$  as predicted by the variational principle.

To illustrate this we consider  $N$  noninteracting, spinless fermions in an external, one-body potential  $v(x) =$

$-8 \sin^2(\pi x)$  in a box, where  $0 < x < 1$ . We perform a variational calculation of the total energy, where we evaluate Eq. (8) in an extremely limited class of trial potentials  $v'(x) = v(x) - \Delta D \sin^2(2\pi x)$ . The result is illustrated in Fig. 7 for  $N = 1$  and  $N = 2$ . The solid black curve depicts the exact calculation with the minimum located at  $\Delta D = 0$ . The dotted (green) curve corresponds to the ISA, which might not even have a minimum, because two independent approximations,  $n_S^A[v]$  and  $T_S^A[v]$ , are employed. The dashed (red) curve is the DSA, which, despite being more accurate, also minimizes not at the true external potential, but at  $\Delta D = 1.2$  for  $N = 1$  and at  $\Delta D = 1.3$  for  $N = 2$ . Furthermore, in Table III we list the total energies given by the exact calculation and absolute errors of several approximations (TF, ISA, and DSA) obtained from the direct evaluation for increasing  $N$ . Additionally, we list the absolute errors of the DSA from the variational calculation along with the effective depth  $\Delta D$  of the minimizing trial potential. This analysis shows that a minimization over some trial potentials can yield a more accurate result at a trial potential different from the true external potential but that this is not always the case; for example, the DSA in Fig. 7 for  $N = 2$  yields a more accurate energy at its variational minimum than at  $\Delta D = 0$ . However, for  $N = 1$  the energy of the DSA at the variational is less accurate. Furthermore,

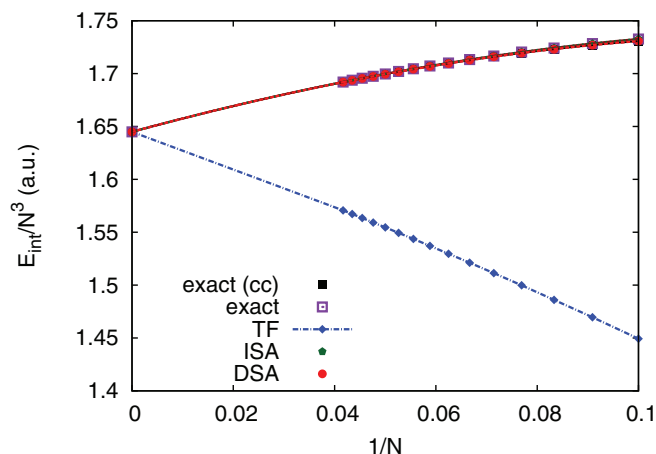


FIG. 5. (Color online) Numerical extraction of leading coefficients in Eq. (64) in the interior from the exact calculation, ISA, and DSA for  $v(x) = -8 \sin^2(\pi x)$ , where the maximum number of particles considered is  $N = 24$ .

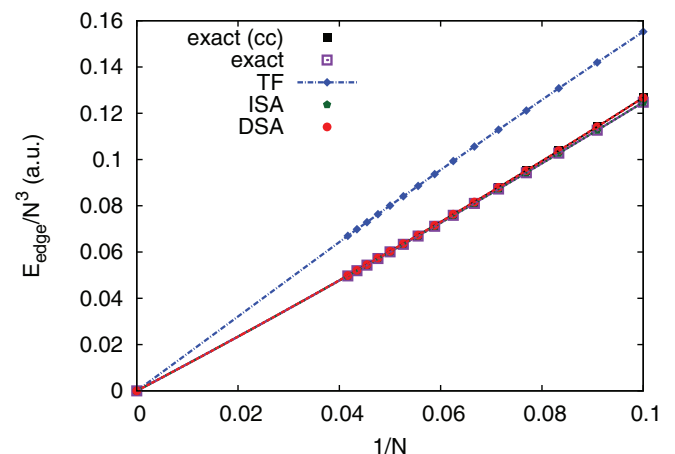


FIG. 6. (Color online) Numerical extraction of the leading coefficients in Eq. (64) close to the edge from the exact calculation, ISA, and DSA for  $v(x) = -8 \sin^2(\pi x)$ , where the maximum number of particles considered is  $N = 24$ .

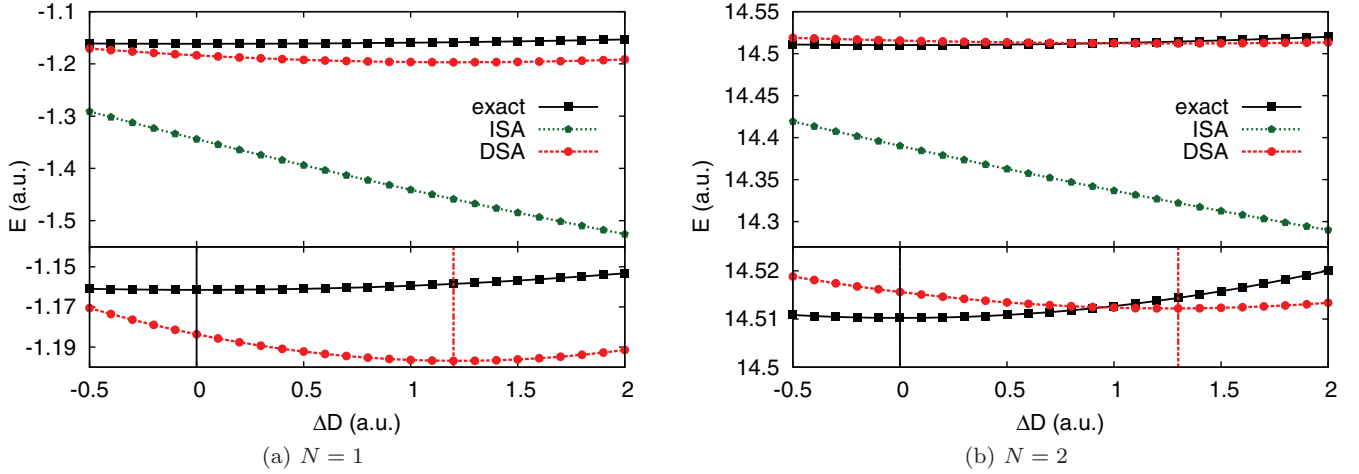


FIG. 7. (Color online) Variational calculation of the total energy [solid (black) line] in comparison to the ISA [dotted (green) line] and the DSA [dashed (red) line] of  $N$  noninteracting, spinless fermions in an external potential,  $v(x) = -8 \sin^2(\pi x)$ , where the minimization is performed over trial potentials  $v'(x) = v(x) - \Delta D \sin^2(2\pi x)$ . Lower panels show a magnification of the exact and the DSA results, illustrating the position of the variational minima.

as  $N$  increases, the error of the DSA decreases quickly, and its variational minimum coincides with the true external potential as demonstrated by the variational results in Table III. Consequently, for large  $N$  a variational minimization of the DSA becomes obsolete, since the minimum will be given at the external potential of the given problem. Furthermore, to find the true global minimum (not guaranteed to exist for a semiclassical expansion, as the DSA is), one needs to search over *all* trial potentials, not just simple multiples of the external potential, which could be achieved via a set of self-consistent equations.

From the previous sections, we know that the DSA's failure to minimize at the correct potential must be caused by its violation of the symmetry condition,

$$\left. \frac{\delta n_S^{\text{sc}}[v](x)}{\delta v(x')} \right|_N = \left. \frac{\delta n_S^{\text{sc}}[v](x')}{\delta v(x)} \right|_N. \quad (69)$$

The specific PFA,  $n_S^{\text{sc}}[v](x) = n_S^{\text{sm}}[v](x) + n_S^{\text{osc}}[v](x)$ , consists of a smooth ( $n_S^{\text{sm}}$ ) and an oscillating ( $n_S^{\text{osc}}$ ) piece [14]. To first order in  $\delta v(x)$  the Fermi energy  $\epsilon_F$  changes as

$$\delta \epsilon_F = \frac{1}{\tau_L} \int_0^L dx \frac{\delta v(x)}{k}, \quad (70)$$

TABLE III. Total energy of  $N$  noninteracting, spinless fermions in the external potential  $v(x) = -8 \sin^2(\pi x)$ , where  $0 \leq x \leq 1$ , and absolute errors of the direct evaluation within the TF, ISA, and DSA. Additionally, we list the absolute errors of the variational evaluation of the DSA together with the minimizing trial potential.

$N$	$E$	Direct			Variational	
		TF	$E^A$ ISA	DSA	$\Delta D$	$E^A$ : DSA
1	-1.161	-1.603	-0.183	-0.022	1.2	-0.038
2	14.510	-9.554	-0.120	0.005	1.3	-0.002
4	129.953	-40.778	-0.036	0.001	0.0	0.001
8	972.652	-162.496	-0.010	$10^{-4}$	0.0	$10^{-4}$

the smooth piece of the density yields

$$\chi_S^{\text{sm}}(x, x') = \frac{1}{\pi k} \left[ \frac{1}{\tau_L p} - \delta(x - x') \right], \quad (71)$$

and the oscillating piece gives

$$\chi_S^{\text{osc}}(x, x') = n^{\text{osc}}(x) [a + b \cot 2\theta - c \cot \alpha], \quad (72)$$

with

$$a = \frac{1}{\tau_L p} \left( \frac{\xi_L}{\tau_L} - \frac{1}{p^2} - \frac{1}{k^2} \right) + \frac{\delta(x - x')}{k^2}, \quad (73)$$

$$b = \frac{2}{p} [\beta - \eta(x - x')], \quad (74)$$

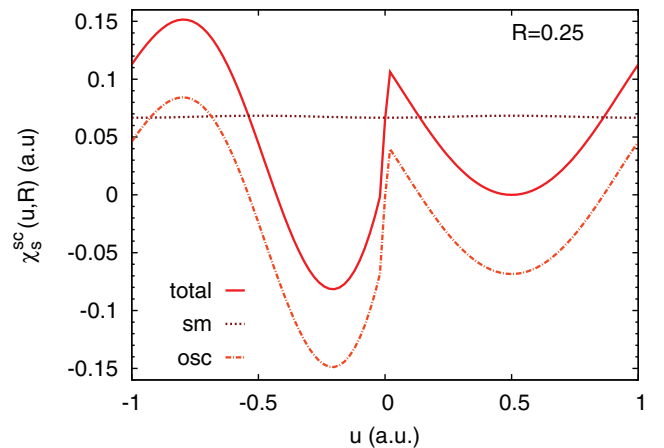


FIG. 8. (Color online) PFA to the static density-density response function for fixed average coordinate  $R = 0.25$  [where  $R = (x + x')/2$ ] as a function of the relative coordinate  $u = x' - x$  of one particle in the external potential  $v(x) = -5 \sin^2 \pi x$ , where  $0 \leq x \leq 1$ . This demonstrates explicitly that Eq. (76) is not symmetric under exchange of coordinates. In particular, we confirm that the smooth (sm) piece given in Eq. (71) is symmetric, whereas the oscillating (osc) piece in Eq. (72) is not.

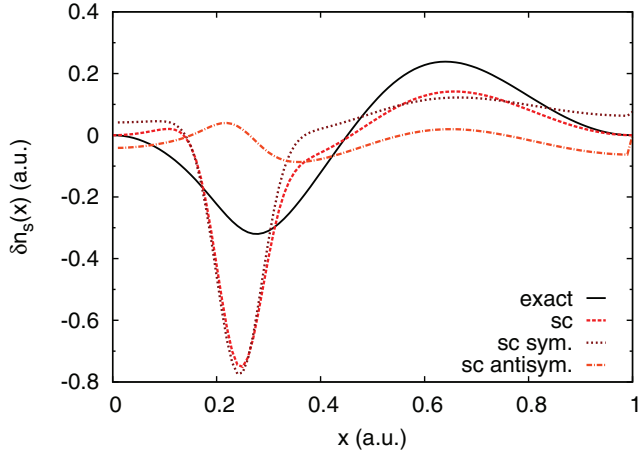


FIG. 9. (Color online) Exact (black) and semiclassical (sc; red) change in density of one particle in the external potential  $v(x) = -5 \sin^2 \pi x$ , due to a change of potential proportional to a Gaussian of width 0.001 centered at  $x = 0.25$ . Symmetric (sc sym.; blue) and antisymmetric (sc antisym.; green) semiclassical contributions are also shown.

$$c = \frac{\pi}{\tau_L p} \left( \frac{\eta(x-x') - \beta}{p^2} + \frac{\beta \xi_L - \xi}{\tau_L} \right), \quad (75)$$

where  $\eta(x-x')$  denotes the Heaviside step function,  $\beta = \tau/\tau_L$ ,  $\xi = -(d\tau/d\epsilon)|_{\epsilon=\epsilon_F}$ , and  $\xi_L = -(d\tau_L/d\epsilon)|_{\epsilon=\epsilon_F}$ . As expected, the functional derivative of the smooth, TF-like piece is symmetric under exchange of  $x$  and  $x'$ . However, the functional derivative of the oscillating piece is *not* symmetric. This is the reason why the DSA curve in Fig. 7 does not minimize at  $v(x)$ .

The fallout of this analysis is an explicit PFA to the static density-density response function,

$$\chi_S^{\text{sc}}[v](x, x') = \chi_S^{\text{sm}}[v](x, x') + \chi_S^{\text{osc}}[v](x, x'), \quad (76)$$

for noninteracting, spinless fermions in an external potential  $v(x)$  confined by box boundaries, which is an interesting result in itself. As an example we consider one particle in  $v(x) = -5 \sin^2 \pi x$ . Introducing average and relative coordinates, i.e.,  $R = (x+x')/2$  and  $u = x' - x$ , we plot Eq. (76) in Fig. 8; this explicitly demonstrates that Eq. (76) is not symmetric under exchange of coordinates. Additionally, in Fig. 9 we illustrate the symmetric and antisymmetric contributions to the change in density  $\delta n_S(x) = \lim_{f \rightarrow 0} (n[v+f v](x) - n[v](x))/f$  calculated via Eq. (76) when the external potential is perturbed by  $\delta v(x) = f g(x)$ , where  $g(x) = \exp[-(x-x_0)^2/(4\sigma)]/(2\sqrt{\pi}\sigma)$ , which approaches a Dirac  $\delta$  function centered at  $x_0$  in the limit  $\sigma \rightarrow 0$ .

## VII. CONCLUSION

In this work, we have established several formal properties of the potential functionals introduced in Ref. [13], especially in terms of their duality to density functionals [11]. We have also shown that the methodology of Ref. [13] can be employed to produce potential functionals more accurate than any that had previously existed. This higher accuracy can be attributed to the “unreasonable utility of asymptotic expansions” [21,22] because the new coupling-constant procedure

considerably improves the accuracy of the asymptotic expansion in powers of  $1/N$ , where  $N$  is the particle number.

Of course, the major drawback of this line of investigation remains: Only in one dimension, and then only for smooth potentials confined by box boundaries, do we have explicit expressions that are uniformly more accurate than TF theory, at the present time. The thrust of the present investigation is to show how promising such approximations are and to dangle the hope of tremendous improvement over present-day density functional approximations, especially for orbital-free calculations.

## ACKNOWLEDGMENTS

A.C. acknowledges Lucas Wagner, Stefano Pittalis, and Raphael Ribeiro of the Burke group for useful comments and proofreading of the manuscript. K.B. and A.C. acknowledge support by the NSF under Grant No. CHE-1112442.

## APPENDIX A: CONFIRMING THE VARIATIONAL PRINCIPLE IN POTENTIAL FUNCTIONAL THOMAS-FERMI THEORY

We show that in noninteracting TF theory the direct evaluation of the total energy in Eq. (47) yields the same result as the minimization over trial potentials given in Eq. (48). If the approximate pair  $\{n_S^{\text{TF}}[v'](\mathbf{r}), F^{\text{TF}}[v']\}$  satisfies the variational principle, i.e.,

$$\frac{\delta}{\delta v'(\mathbf{r})} \left( F^{\text{TF}}[v'] + \int d^3r \{v(\mathbf{r}) - \mu\} n_S^{\text{TF}}[v'](\mathbf{r}) \right) = 0, \quad (A1)$$

then the statement above is true. To confirm the latter, define the local chemical potential  $\tilde{\mu}[v](\mathbf{r}) = \mu - v(\mathbf{r})$ , which is directly related to the density via

$$n_S^{\text{TF}}[v](\mathbf{r}) = \frac{\{2\tilde{\mu}[v](\mathbf{r})\}^{3/2}}{3\pi^2}. \quad (A2)$$

Take the functional derivative in Eq. (A1) using the chain rule, e.g.,

$$\frac{\delta T_S^{\text{TF}}}{\delta v'(\mathbf{r})} = \int d^3r' \frac{\delta T_S^{\text{TF}}}{\delta \tilde{\mu}(\mathbf{r}')} \frac{\delta \tilde{\mu}(\mathbf{r}')}{\delta v'(\mathbf{r})}, \quad (A3)$$

considering that

$$\frac{\delta \tilde{\mu}(\mathbf{r}')}{\delta v'(\mathbf{r})} = -\delta(\mathbf{r}' - \mathbf{r}), \quad (A4)$$

where  $\delta(\mathbf{r}' - \mathbf{r})$  denotes the Dirac  $\delta$  function, and keeping the chemical potential  $\mu$  fixed, since it is determined at the end of the minimization by requiring normalization. Then we find that  $v'(\mathbf{r}) = v(\mathbf{r})$ , as expected.

## APPENDIX B: WALLS AT INFINITY

The DSA can be applied to potentials for which  $v(x) \rightarrow 0$  as  $|x| \rightarrow \infty$  and where  $v_0 = 0$  is chosen as a reference potential. However, for this choice the coupling-constant integral in Eqs. (12) and (23) might be undefined, because the particle number may change abruptly with the coupling constant. To assure the existence of the coupling-constant integral, we use

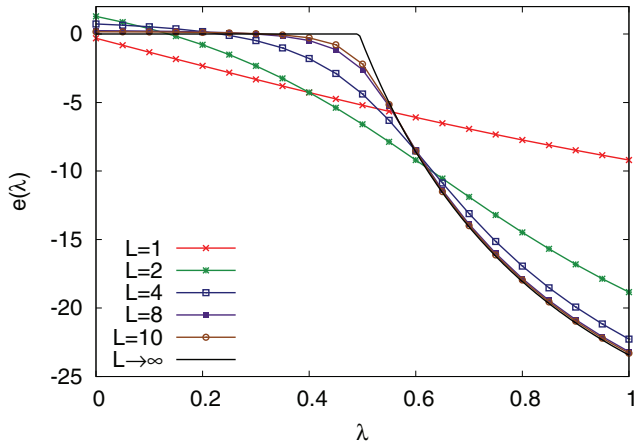


FIG. 10. (Color online) Plot of  $e(\lambda)$  for the second level as a function of the coupling constant  $\lambda$  and for different values of  $L$  denoting the distance between the hard walls.

the formal device of introducing hard walls and taking the limit of infinite separation at the end of the calculation.

We demonstrate this procedure for a simple case. Consider  $v(x)$  to be a finite square well. Assume that the depth of the square well is such that there are two bound states. When the coupling-constant integral is performed the depth of the well changes from its initial value at  $\lambda = 1$  to 0 at  $\lambda = 0$ . As the depth decreases, there is a point where the energy of the second bound state passes through 0 and vanishes. For values smaller than this critical value of  $\lambda$  the integrand of the coupling-constant integral is not defined and therefore cannot be applied. To cure this problem we introduce hard walls separated by a distance  $L$  as a reference potential. Thus, all levels in the well stay bound and the integrand is defined for the entire range  $\lambda \in [0, 1]$ . By taking the limit  $L \rightarrow \infty$  the coupling-constant calculation converges to the case where only the original potential  $v(x)$  is present. We demonstrate this explicitly by calculating the quantity

$$e(\lambda) = E_0(L) + \int_{-L/2}^{L/2} dx n[v^\lambda](x) v(x) \quad (\text{B1})$$

for the second bound state and a well depth of 40. This is the  $\lambda$ -dependent integrand of Eq. (11), with  $E_0(L) = 4\pi^2/(2L^2)$  denoting the reference energy of the second bound state in an infinite square well; integrating  $e(\lambda)$  over the coupling constant yields the orbital energy of the second bound state. We plot  $e(\lambda)$  for increasing  $L$  in Fig. 10: the critical value of  $\lambda$ , below which the second level vanishes, is indicated by the kneelike feature at  $\lambda \approx 0.5$ . The calculation in the simulation box converges to the exact result of the finite square well in a continuous

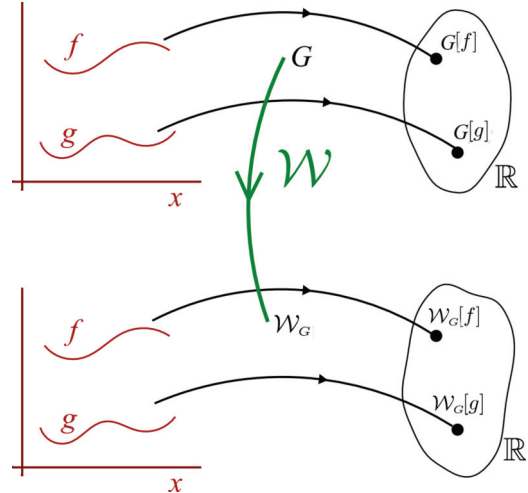


FIG. 11. (Color online) Schematic illustrating the concept of a ffunctional.

manner as the separation between the walls is made larger. This demonstrates how, in principle, the DSA can be applied for potentials that vanish at infinity but also shows that the coupling-constant dependence may become quite strong.

### APPENDIX C: DEFINITION OF A FFUNCTIONAL

Here we explain the meaning of the term *ffunctional*, which first appears as  $\mathcal{F}_n^{\text{cc}}[v]$  in Eq. (12), where we introduce the universal functional in terms of a coupling-constant expression. Simply speaking, a ffunctional maps a functional to a functional; e.g.,  $\mathcal{F}_n^{\text{cc}}[v]$  takes the functional  $n[w](\mathbf{r})$ —the density as a functional of some potential  $w(\mathbf{r})$ —and creates a new functional of the external potential.

To understand this concept consider the schematic in Fig. 11 and the following example: Assume a particular ffunctional that is defined as

$$\mathcal{W}_G[f] = \int_{-\infty}^{\infty} d^3r f^\alpha(\mathbf{r}) \quad (\text{C1})$$

with  $\alpha = \int_0^1 d\lambda G[\lambda q]$ . Now for a given functional  $G[q]$ , such as

$$G[q] = \int_{-\infty}^{\infty} d^3r q^2(\mathbf{r}), \quad (\text{C2})$$

for which  $\alpha = \int_{-\infty}^{\infty} d^3r q^2(\mathbf{r})/3$  [assuming a well-behaved function  $q(\mathbf{r})$ ], the ffunctional  $\mathcal{W}$  maps  $G[q]$  to  $\mathcal{W}_G[q]$ . However, a different choice of  $G[q]$  would have resulted in a different  $\mathcal{W}_G$ .

- [1] W. Kohn and L. J. Sham, *Phys. Rev.* **140**, A1133 (1965).  
 [2] A. D. Becke, *Phys. Rev. A* **38**, 3098 (1988).  
 [3] C. Lee, W. Yang, and R. G. Parr, *Phys. Rev. B* **37**, 785 (1988).  
 [4] A. D. Becke, *J. Chem. Phys.* **98**, 5648 (1993).  
 [5] J. P. Perdew, K. Burke, and M. Ernzerhof, *Phys. Rev. Lett.* **77**, 3865 (1996); **78**, 1396(E) (1997).

- [6] D. Rappoport, N. R. M. Crawford, F. Furche, and K. Burke, in *Computational Inorganic and Bioinorganic Chemistry*, edited by E. Solomon, R. King, and R. Scott (John Wiley & Sons, New York, 2009).  
 [7] B.-G. Englert and J. Schwinger, *Phys. Rev. A* **29**, 2339 (1984).

- [8] L. H. Thomas, *Math. Proc. Cambr. Phil. Soc.* **23**, 542 (1927).
- [9] E. Fermi, *Z. Phys. A* **48**, 73 (1928).
- [10] B.-G. Englert, *Phys. Rev. A* **45**, 127 (1992).
- [11] W. Yang, P. W. Ayers, and Q. Wu, *Phys. Rev. Lett.* **92**, 146404 (2004).
- [12] E. K. U. Gross and C. R. Proetto, *J. Chem. Theory Comput.* **5**, 844 (2009).
- [13] A. Cangi, D. Lee, P. Elliott, K. Burke, and E. K. U. Gross, *Phys. Rev. Lett.* **106**, 236404 (2011).
- [14] P. Elliott, D. Lee, A. Cangi, and K. Burke, *Phys. Rev. Lett.* **100**, 256406 (2008).
- [15] A. Cangi, D. Lee, P. Elliott, and K. Burke, *Phys. Rev. B* **81**, 235128 (2010).
- [16] M. Levy, *Phys. Rev. A* **26**, 1200 (1982).
- [17] E. H. Lieb, *Int. J. Quantum Chem.* **24**, 243 (1983).
- [18] P. Hohenberg and W. Kohn, *Phys. Rev.* **136**, B864 (1964).
- [19] D. A. Kirzhnits, *Sov. Phys. JETP* **5**, 64 (1957).
- [20] P. R. Antoniewicz and L. Kleinman, *Phys. Rev. B* **31**, 6779 (1985).
- [21] J. Schwinger, *Phys. Rev. A* **22**, 1827 (1980).
- [22] J. Schwinger, *Phys. Rev. A* **24**, 2353 (1981).
- [23] K. Burke, J. P. Perdew, and M. Ernzerhof, *J. Chem. Phys.* **109**, 3760 (1998).
- [24] F. G. Cruz, K.-C. Lam, and K. Burke, *J. Phys. Chem. A* **102**, 4911 (1998).
- [25] K. Burke, F. G. Cruz, and K.-C. Lam, *J. Chem. Phys.* **109**, 8161 (1998).
- [26] J. Tao, V. N. Staroverov, G. E. Scuseria, and J. P. Perdew, *Phys. Rev. A* **77**, 012509 (2008).
- [27] M. Levy, *Proc. Natl. Acad. Sci. USA* **76**, 6062 (1979).
- [28] E. H. Lieb, *Physics as Natural Philosophy* (MIT Press, Cambridge, MA, 1982), p. 111.
- [29] R. M. Dreizler and E. K. U. Gross, *Density Functional Theory: An Approach to the Quantum Many-Body Problem* (Springer-Verlag, New York, 1990).
- [30] R. F. Nalewajski and R. G. Parr, *J. Chem. Phys.* **77**, 399 (1982).
- [31] B.-G. Englert, *Lect. Notes Phys.* **300**, 110 (1988).
- [32] E. Sim, J. Larkin, K. Burke, and C. Bock, *J. Chem. Phys.* **118**, 8140 (2003).
- [33] D. Lee, A. Cangi, P. Elliott, and K. Burke (unpublished).
- [34] A. Cangi, S. Pittalis, C. R. Proetto, E. K. U. Gross, and K. Burke (unpublished).
- [35] J. Goodisman, *Phys. Rev. A* **2**, 1 (1970).
- [36] D. Eimerl, *J. Math. Phys.* **18**, 106 (1977).
- [37] G. F. Kventsel and J. Katriel, *Phys. Rev. A* **24**, 2299 (1981).
- [38] S. Kobayashi, T. Matsukuma, S. Nagai, and K. Umeda, *J. Phys. Soc. Japan* **10**, 759 (1955).
- [39] See Supplemental Material at <http://link.aps.org/supplemental/10.1103/PhysRevA.88.062505> for details of the asymptotic analysis in Sec. V.
- [40] K. Burke, J. P. Perdew, and Y. Wang, in *Electronic Density Functional Theory: Recent Progress and New Directions*, edited by J. F. Dobson, G. Vignale, and M. P. Das (Plenum Press, New York, 1997), p. 81.
- [41] A. V. Arbuznikov and M. Kaupp, *J. Chem. Phys.* **136**, 014111 (2012).